General Disclaimer

One or more of the Following Statements may affect this Document

- This document has been reproduced from the best copy furnished by the organizational source. It is being released in the interest of making available as much information as possible.

- This document may contain data, which exceeds the sheet parameters. It was furnished in this condition by the organizational source and is the best copy available.

- This document may contain tone-on-tone or color graphs, charts and/or pictures, which have been reproduced in black and white.

- This document is paginated as submitted by the original source.

- Portions of this document are not fully legible due to the historical nature of some of the material. However, it is the best reproduction available from the original submission.

8.0 - 1 0 2 3 5
TM - 81631

NASA

Technical Memorandum 80631

(E80-10235) REMOTE SENSING OF TOTAL DRY-MATTER ACCUMULATION IN WINTER WHEAT (NASA) 28 p HC A03/MF A01 CSCL 02C

N80-29804

Unclas
G3/43 00235

REMOTE SENSING OF TOTAL DRY-MATTER ACCUMULATION IN WINTER WHEAT

Compton J. Tucker, Brent N. Holben,
James H. Elgin, Jr., and James E. McMurtrey, III

JANUARY 1980

National Aeronautics and
Space Administration

Goddard Space Flight Center
Greenbelt, Maryland 20771

REMOTE SENSING OF TOTAL DRY-MATTER ACCUMULATION IN WINTER WHEAT

Compton J. Tucker, Brent N. Holben, James H. Elgin, Jr.,
and James E. McMurtrey, III

January 1980

GODDARD SPACE FLIGHT CENTER
Greenbelt, Maryland

REMOTE SENSING OF TOTAL DRY-MATTER ACCUMULATION IN WINTER WHEAT*

Compton J. Tucker and Brent N. Holben
NASA/Goddard Space Flight Center
Greenbelt, Maryland 20771 USA

James H. Elgin, Jr. and James E. McMurtrey, III
USDA-SEA-AR/Beltsville Agricultural Research Center
Beltsville, Maryland 20705 USA

ABSTRACT

Red and photographic-infrared spectral data collected on 21 dates over the growing season with a hand-held radiometer were quantitatively correlated with total dry-matter accumulation in winter wheat. The spectral data were found to be highly related to vigor and condition of the plant canopy. Two periods of drought stress and subsequent recovery from it were readily apparent in the spectral data. Simple ratios of the spectral radiance data compensated for variations in solar intensities and, when integrated over the growing season, explained 79% of the variation in total above-ground accumulation of dry matter. A satellite system is proposed to provide large-area assessment of total dry accumulation or net primary production from terrestrial vegetation.

*This is a preprint submitted to Remote Sensing of Environment

REMOTE SENSING OF TOTAL DRY-MATTER ACCUMULATION IN WINTER WHEAT

INTRODUCTION

The global carbon dioxide (CO_2) cycle has been the subject of much recent interest and continues to be the subject of serious international concern (Andersen and Malahoff, 1977; Baes et al., 1976; Bolin, 1970; Bolin et al., 1979; Bohn, 1976; Keeling, 1973; Keeling et al., 1976a and b; Rotty, 1977; Rotty, 1978; SCEP, 1979; Schlesinger, 1979; Stuiver, 1978; Whittaker and Likens, 1975; Williams, 1978; Woodwell and Houghton, 1977; Woodwell and Pecan, 1973; Woodwell et al., 1978; Woodwell, 1978).

Remote sensing, with its unique synoptic perspective, has been mentioned as a possible means of monitoring the terrestrial vegetation biomass or phytomass. The role of the phytomass in the global CO_2 cycle is extremely important and involves the amount of carbon stored in various plant communities of the world, with special emphasis on forested areas and, in particular, tropical forests (Atjay et al., 1979; Bolin, 1977; Lemon, 1977; Rodin et al., 1975; Whittaker and Likens, 1975; Woodwell and Houghton, 1977; Woodwell and Pecan, 1973; Woodwell et al., 1978; Woodwell, 1978). Remote sensing techniques might be employed in attempts to satisfy three interrelated requirements for information about the terrestrial phytomass: the distribution of the various plant communities; changes in the distribution of the plant communities with time and, particularly, deforestation; and the net primary productivity of the various plant communities, including regrowth following deforestation. Remote sensing unfortunately cannot be used for direct measurement of the carbon stored as above-ground phytomass.

Numerous studies have shown that remote sensing can be used to accurately map vegetation and land-use types (Anuta and MacDonald, 1971; Bauer, 1975; Bauer et al., 1979; Bizzell et al., 1975; Hay, 1974; Kettig and Landgrebe, 1976; Kumar and Silva, 1977; MacDonald et al., 1972; MacDonald and Hall, 1977; Morian and Williams, 1975; Steiner, 1970), to monitor plant growth and development through the high correlation of spectral data with the green-leaf biomass or green-leaf area (Holben et al., 1980; Kimes et al., 1980; Wiegand et al., 1979), and to monitor deforestation in various forest types (Miller and Williams, 1978).

Several studies have shown that currently used remote-sensing techniques are not sensitive to stems, wood, dead vegetation, or other non-green-leaf biomass components of plant canopies (Holben et al., 1980; Kimes et al., 1980; Tucker, 1979). Although new remote-sensing techniques might in subsequent years enable the direct assessment of the above-ground phytomass carbon world-wide, the possibility of developing such techniques must be considered tenuous at best. This report is restricted to what is currently thought will be possible in the 1980's and 1990's.

We report herein on a technique that can be used to assess net primary productivity or total dry-matter accumulation from frequently collected red and photographic-infrared spectral data for winter wheat canopies. The same technique is thought to be extendable to terrestrial vegetaion in general.

BACKGROUND

Of all the techniques for monitoring vegetation evaluated to date, the use of red (0.60-0.70μm) and near-infrared (0.75-1.1 μm) spectral data has had the most applications with a variety of vegetation types. These data have been used to estimate the leaf-area index of tropical rain forests (Jordan, 1969), the green-leaf area and biomass of soybeans (Holben et al., 1980) and winter wheat (Wiegand et al., 1979), estimate forage biomass (Pearson and Miller, 1972; Rouse et al., 1973; Colwell, 1974; Carneggie et al., 1974; Deering et al., 1975; Pearson et al., 1976b; Maxwell, 1976; Tucker et al., 1979a), monitor greenwave effects in the hardwood forest (Ashley and Rea, 1975; Blair and Baumgardner, 1977), predict grain yield (Colwell et al., 1977; Tucker et al., 1980b; Pinter et al., 1979), monitor crop condition (Richardson and Wiegand, 1977; Tucker et al., 1980b), and estimate the severity of drought stress (Thompson and Wehmanen, 1979; Tucker et al., 1980a). A review of these techniques is given in Tucker (1979).

Spectral reflectances and radiances in the red region of the electromagnetic spectrum are inversely related to the in situ chlorophyll density, while spectral reflectances and radiances in the near infrared region are directly related to the green leaf density (Gates et al., 1965; Knipling, 1970; Woolley, 1971).

If one avoids the 0.70-0.74 μm region, which is not sensitive to green vegetation (Tucker and Maxwell, 1976), and also avoids near infrared water-vapor-absorption bands at ~0.76-0.77 and ~0.92-0.98 μm (Frasier, 1975), the result is a near infrared sensor in the 0.77-0.91 μm region with atmospheric absorption/transmission properties similar to those of the 0.60-0.70 μm region in addition to being highly sensitive to the green-leaf density. Variation(s) in the spectral quality between the 0.60-0.70 and 0.77-0.91 μm bands are minimized because of their close spectral proximity and similar atmospheric absorption/transmission properties. Simple radiance ratios of these two bands can therefore be used to effectively compensate for first order variation in the solar spectral irradiance. These circumstances, coupled with the strong and different relationships of these data to green-plant canopies, are responsible for the usefulness of these data for monitoring vegetation.

EXPERIMENTAL PROCEDURES

Our experiment was conducted in a 1.2-ha soft red winter wheat (Triticum aestivum L.) field at the Beltsville Agricultural Research Center, Beltsville, Maryland. The field was plowed, disked, and planted with the cultivar "Arthur" on October 6, 1977, at a seeding rate of 107.6 kg/ha. The seeding was done with a conventional grain drill, with 17.8 cm between rows. Before seeding the field was limed according to soil-test recommendations and fertilized with N at 33.3 kg/ha, P at 53.8 kg/ha, and K at 53.8 kg/ha. The following spring (early March 1978) the crop was topdressed with N at 20.4 kg/ha.

Twenty 2- X 3-m plots in the wheat field were selected during the winter dormant period. Four pairs of red and photographic-infrared spectral measurements were taken per plot with a hand-held digital radiometer (Pearson et al., 1976a). Data were collected on 21 dates between March 21, 1978 (Julian date 80), and June 23, 1978 (Julian date 174), at intervals ranging from 1 to 9 days (Table 1).

The red (0.65-0.70 μm) and photographic-infrared (0.775-0.825 μm) spectral-radiance data were used to form the IR/red ratio and the normalized difference (ND) of Rouse et al. (1973) and Deering et al., (1975), where:

$$ND = (IR - red)/(IR + red) \quad (1)$$

Table 1
Tabular Listing of the Days when Hand-Held Radiometer Data were Collected from the 20 2 × 3 m Winter Wheat Plots in 1978

Sampling Sequence	Julian Date	Time (EST)	Conditions/Comments (Temperature, Sky, Wind, Etc.)
1	80	1130-1215	12°C, clear with no clouds, wind = 16 kmh
2	89	1215-1300	8°C, clear with no clouds, calm, soil damp
3	92	1222-1310	15°C, clear with no clouds, calm
4	95	1220-1245	17°C, a few scattered clouds, wind = ~5-10 kmh
5	97	1225-1247	21°C, a few scattered clouds, calm
6	102	1110-1135	14°C, clear with no clouds, wind = ~5 kmh
7	104	1210-1230	20°C, clear with no clouds, wind = 30-45 kmh
8	112	1338-1415	18°C, scattered clouds, gusty wind = 5-20 kmh
9	118	1230-1310	22°C, clear with no clouds, gusty wind = 5-30 kmh
10	121	1200-1230	16°C, clear with no clouds, wind = 5-10 kmh
11	123	1215-1250	18°C, clear with no clouds, calm
12	131	1145-1210	24°C, a few scattered clouds, wind = ~10 kmh
13	139	1145-1230	20°C, a few scattered clouds, wind = <15 kmh
14	146	1125-1205	19°C, a few scattered clouds, calm
15	152	1130-1200	22°C, clear with no clouds, wind = 5-10 kmh
16	157	1050-1120	22°C, a few scattered clouds, wind = ~10 kmh
17	161	1230-1300	26°C, clear with no clouds, calm
18	165	1030-1125	17°C, a few scattered clouds, wind = 25-40 kmh
19	166	1100-1200	20°C, high faint cirrus, calm
20	170	1030-1100	20°C, a few scattered clouds, wind = <10 kmh
21	174	1100-1130	28°C, clear with no clouds, calm

Mean time between sampling dates = 4.7 days
Range between sampling dates = 1-9 days
Medium time between sampling dates = 4,5 days (tie)
Table 1 from Tucker et al., 1980b.

The four pairs of spectral measurements per plot were averaged to account for the spatial variability present in each plot. All spectral data were collected under sunny skies within plus or minus 90 minutes of local solar noon, and measured normal to the ground surface (Table 1).

Throughout the growing season average plant height, estimated percentage of cover, and phenological development were recorded for the field area (Table 2). The crop reached harvest maturity in late June 1978. On June 28, 1978 (Julian date 179), a 0.9- × 3.0-m swath was cut from the center of each plot with a small sickle-bar mower. Total biomass and grain yield were recorded. Grain yield data were reported by Tucker et al. (1980b). The entire above-ground biomass was oven dried at 60°C for 72 hours and weighed; the resulting total dry-matter accumulation was expressed in g/m^2.

Table 2
Agronomic Data Pertaining to Average Plant Heights, Estimated Percentage Canopy Cover, and Crop Growth Stages at 10 Selected Dates for 20 Winter Wheat Plots (1978)

Calendar Date	Julian Date	Plant Height (cm)	Percentage Cover	Growth Stages: Numerical (after Zadoks et al., 1974)	Growth Stages: Descriptive
04/24/78	114	35.0	54	34	stem elongation, 4th node detectable
05/01/78	121	45.2	56	35	stem elongation, 5th node detectable
05/11/78	131	70.8	66	44	booting, boots just visible
05/19/78	139	90.8	64	58	inflorescence emerges
05/25/78	145	112.0	68	64	anthesis, half-way
06/01/78	152	112.5	61	73	early milk
06/06/78	157	114.8	63	85	soft dough
06/14/78	165	115.5	64	85	soft dough
06/20/78	171	111.8	51	87	hard dough
06/23/78	174	108.5	51	89	hard dough
06/27/78	178	104.0	51	92	ready for harvest

Table 2 from Tucker et al., 1980b.

The data on average red radiance, IR radiances, IR/red ratio, and ND for each plot were regressed on the total dry-matter accumulation at the end of the season separately for each of the 21 sampling dates. In addition, the IR/red ratio and the ND were integrated over Julian sampling dates and regressed on total dry-matter accumulation.

RESULTS AND DISCUSSION

Examples of the radiance data and irradiance normalizing ratios were first plotted against Julian date (Figure 1). The red radiance plotted against Julian date showed the effect of increasing chlorophyll absorption (decreasing radiance) to about Julian date 139, when the onset of senescence resulted in progressively higher levels of radiance (Figure 1a) [(lower levels of absorption)]. The photographic-infrared radiance, in contrast, gradually increased with time to about Julian date 139, when the onset of senescence resulted in progressively lower levels of radiance in this band (Figure 1b). This change resulted from the direct relationship of the photographic infrared radiance to the green leaf density of the wheat canopy. The IR/red radiance ratio and the ND both exhibited similar trends with respect to Julian date (Figures 1c and 1d, respectively.)

The trends with respect to Julian date for IR/red radiance ratio and the ND for our 20 plots were similar in character (Figure 2). Five component trends were apparent with respect to Julian date: (1) Both the IR/red radiance ratio and the ND increased as the spring portion of the growing season began, but the rate of increase diminished as Julian date 102 approached; (2) Both spectral variables increased rapidly between Julian dates 102 and 112 because of precipitation on Julian dates 102-104; (3) Both spectral variables declined from Julian dates 112-123, when precipitation was lacking; (4) Heavy rains on Julian dates 124-127 and 132-136 resulted in increases in both the IR/red radiance ratio and the ND; (5) Late-season senescence caused a decrease in both the IR/red radiance ratio and the ND approximately between Julian dates 139 and 175 (this decrease resulted from chlorophyll breakdown and the loss of green leaf area in the wheat canopy, and was visually perceptible as a gradual yellowing of the wheat canopy.) We observed these same five temporal trends in various degrees for all of our 20 experimental plots.

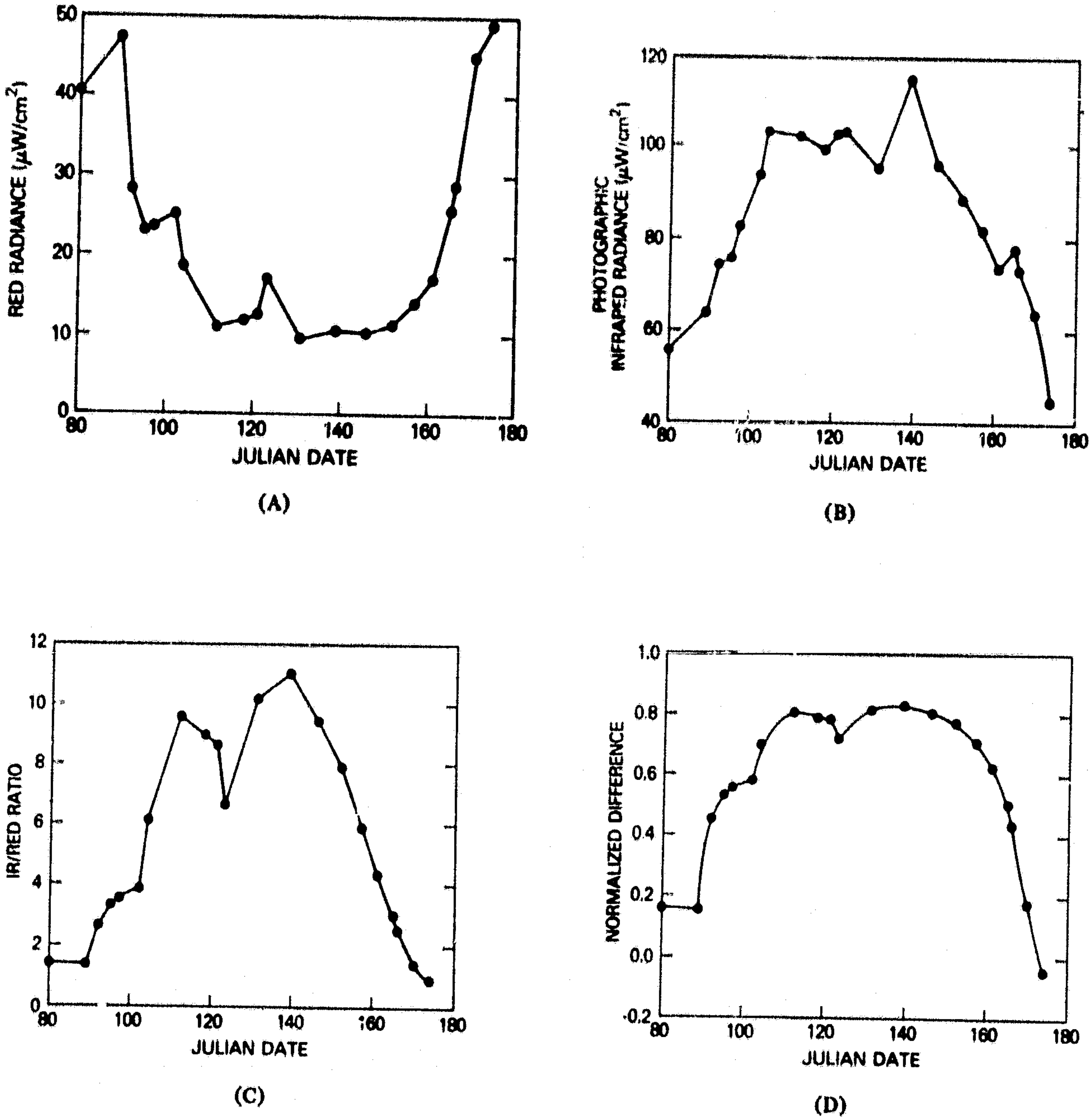

Figure 1. (A) Red radiance; (B) Photographic infrared radiance; (C) IR/red radiance ratio; and (D) the normalized difference (ND) plotted against Julian date for one of 20 wheat plots sampled. Note how the IR/red radiance ratio and the normalized difference effectively compensate for the variability present in the radiance data. (Figure 1 from Tucker et al., 1980b)

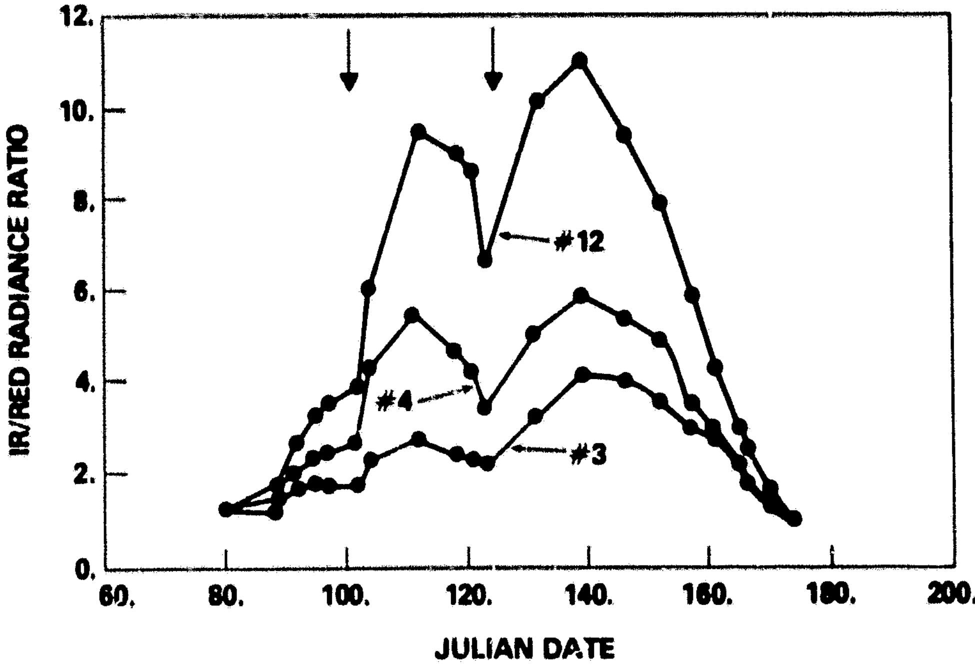

(A)

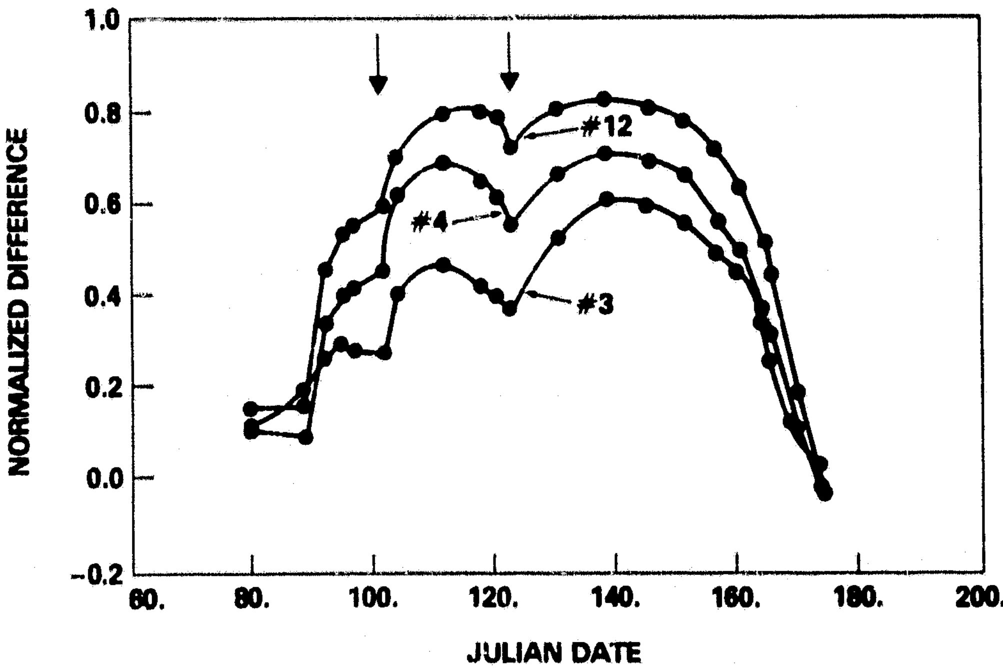

(B)

Figure 2. The IR/red radiance ratio (A) and the normalized difference (B) from three 2 X 3 m plots plotted against Julian date. The vertical arrows represent episodes of rainfall. Note the response of the two spectral variables to the occurrence of precipitation which ended periods of water stress. (Figure 2 from Tucker et al., 1980b)

The modulation of the IR/red radiance ratio and ND with respect to precipitation was an example of spectral detection of wheat-canopy water stress and was consistent with previously published results (Thompson and Wehmanen, 1979; Tucker et al., 1980a). Factors that adversely affect plant growth and development are readily apparent in the spectral data if they affect either the chlorophyll density or the green-leaf biomass. Transient wheat-canopy water stress in this case was expressed spectrally largely because of a reduction in the leaf chlorophyll density. The spectral expression of this reduction was apparent in Figure 1a: the increase in the 0.65-0.70 μm radiance (i.e., decrease in absorption) for Julian dates 102 and 123 corresponded to the relative maximum for each of the two episodes of water stress. The 0.775-0.824 μm radiance, in contrast, was not as greatly affected by the episodes of transient water stress (Figure 1b). These differences implied that the green-leaf area remained fairly constant while the leaf chlorophyll density was temporarily reduced, either through photooxidation, enzymatic activity, or some other reducing mechanism (Tucker et al., 1975; Tucker et al., 1980a). The possibility that canopy geometry changes with water stress must also be considered, although visual signs of wilting were not readily apparent.

The next phase of the analysis was the regression of the spectral data on the total dry-matter accumulation sampled at the end of the growing season for each of the 21 sampling dates (Figure 3, Table 3). Correlation coefficients were small and often not significant for the first four sampling dates; however correlation coefficients for dates 5 through 9 were highly significant (note the marked decrease in the correlation coefficient at sampling date 7, which was attributed to high winds [see Table 1]). Correlation coefficients declined for dates 20 and 21 (Table 3) as senescence progressed.

We observed a 45-day period (between Julian dates 112 and 157) in which our spectral data were more highly and significantly correlated to the total dry-matter accumulation than they were earlier in the growing season (Figure 4, Table 3). However, the predicted regression relationships were not constant during this period (Table 4). This variation indicated that a different remote sensing approach was needed.

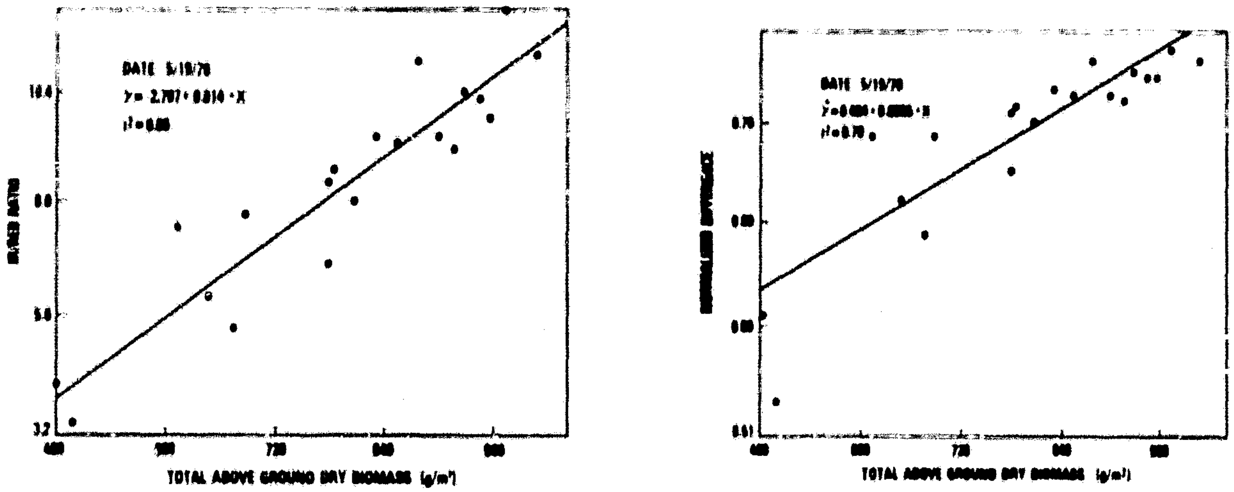

(A) (B)

Figure 3. The IR/red radiance ratio and normalized difference plotted against total above-ground dry matter accumulation on May 19, 1978 (Julian date 139). The total dry matter accumulations were sampled at the end of the growing season.

Inspection of Figure 2 indicated that spectral data such as ours need to be collected often enough that they accurately represent the dynamic nature of plant canopy growth and development in response to environmental conditions. The character of our spectral data, which literally reflected the wheat canopy's vigor and condition, would be substantially different with an average interval of 9 or 18 days, instead of 4.7, between sampling dates.

We next evaluated integrating the red and photographic-infrared spectral data over Julian dates. Comparison of the data in Figure 2 with precipitation data showed that the IR/red radiance ratio and the ND increased when conditions were favorable, so these ratios thus appear to represent the wheat canopy vigor. Therefore, by integrating these data over Julian dates, we were able to summarize the growing-season dynamics for the wheat plots in our study (Figures 5 and 6). Using this technique we found that IR/red radiance ratio and ND, integrated over all Julian sampling dates, explained 76% and 79%, respectively, of the variation in total dry-matter accumulation.

It should be noted that the spectral data in our study were correlated only with the above-ground total dry biomass. Plants suffering from water-uptake deficiencies have been reported to allocate proportionally more of their growth below ground and less above ground than plants of the same

Table 3
Correlation Coefficients for the Four Radiance Variables and Total Dry Matter Accumulation for Each of the 21 Days where Spectral Data were Collected in 1978 for the 20 Winter Wheat Plots. Refer also to Figure 4.

Sampling Sequence	Julian Date	Red Radiance	IR Radiance	IR/Red Radiance Ratio	Normalized Difference
1	80	0.23	0.55*	0.23	0.23
2	89	-0.45*	0.58**	0.53*	0.54*
3	92	-0.26	0.46*	0.38	0.35
4	95	-0.41	0.46*	0.53*	0.50*
5	97	-0.84**	0.88**	0.80**	0.88**
6	102	-0.83**	0.88**	0.78**	0.86**
7	104	-0.54*	0.70**	0.64**	0.62**
8	112	-0.81**	0.85*	0.81**	0.84**
9	118	-.88**	0.82**	0.82**	0.89**
10	121	-0.88	0.74**	0.88**	0.91**
11	123	-0.85**	0.82**	0.82**	0.88**
12	131	-0.84**	0.84**	0.85**	0.86**
13	139	-0.85**	0.91**	0.93**	0.88**
14	146	-0.79**	0.89**	0.86**	0.83**
15	152	-0.82**	0.77**	0.83**	0.83**
16	157	-0.80**	0.73**	0.80**	0.81**
17	161	-0.60**	0.77**	0.72**	0.71**
18	165	-0.54*	0.56*	0.61**	0.59**
19	166	-0.59**	0.47*	0.62**	0.61**
20	170	0.16	0.44*	0.29	0.27
21	174	0.50*	-0.19	-0.55*	-0.54*

*Significant at the .05 level of probability

**Significant at the .01 level of probability

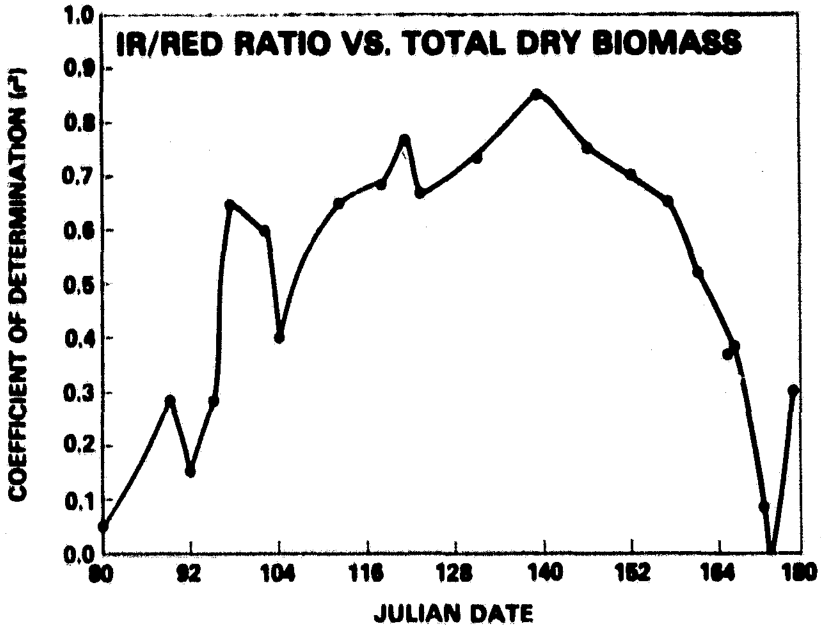

(A)

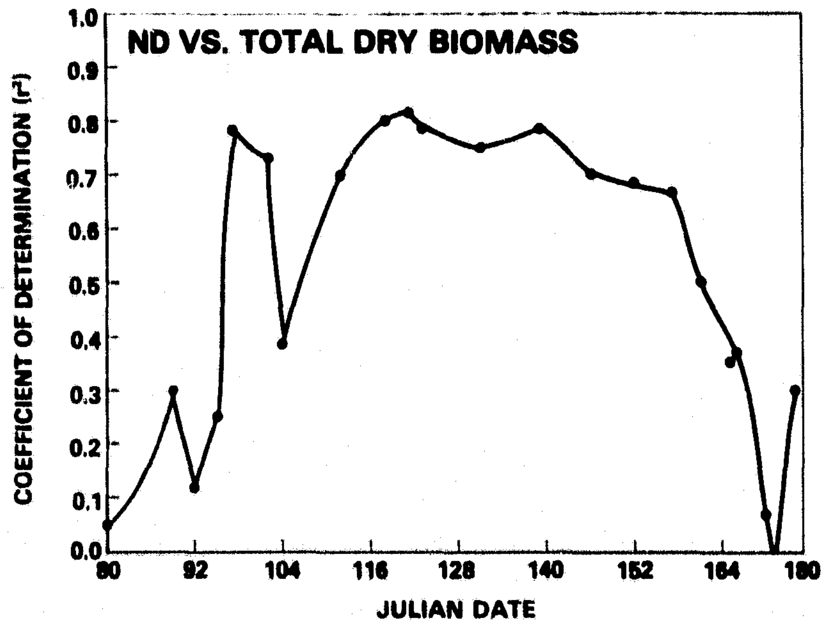

(B)

Figure 4. Coefficients of determination resulting from regressing the (A) IR/red radiance ratio or (B) normalized difference against total dry matter accumulation for each of the 21 data collection dates. The r^2 values presented in Figure 4 are plotted against Julian date along with respective r^2 values for the other 20 dates. Note how the normalized difference was more highly correlated to total dry matter accumulation than was the IR/red radiance ratio earlier in the growing season.

Table 4
Derived Estimates for β_0 and β_1 for Julian dates 112–157 using the IR/Red Radiance Ratio and the Normalized Difference to Predict Total Dry Matter Accumulation. The Equation Used was of the Form TOTAL DRY MATTER $(g/m^2) = \beta_0 + \beta_1$ (Spectral Variable).

Sampling Period	Julian Date	IR/RED Radiance Ratio			Normalized Difference		
		β_0	β_1	r^2	β_0	β_1	r^2
8	112	486.6	56.4	0.65	−51.1	1298.5	0.71
9	118	511.0	57.1	0.68	7.0	1258.3	0.80
10	121	483.2	57.5	0.77	36.8	1188.3	0.82
11	123	494.6	68.8	0.67	96.2	1189.0	0.78
12	1[illegible]1	424.2	56.8	0.73	−258.4	1506.1	0.74
13	139	306.2	65.7	0.86	−560.8	1848.5	0.78
14	146	297.7	79.4	0.74	−414.5	1733.3	0.69
15	152	243.9	102.2	0.69	−416.8	1885.8	0.69
16	157	275.4	133.35	0.64	−199.0	1730.5	0.66

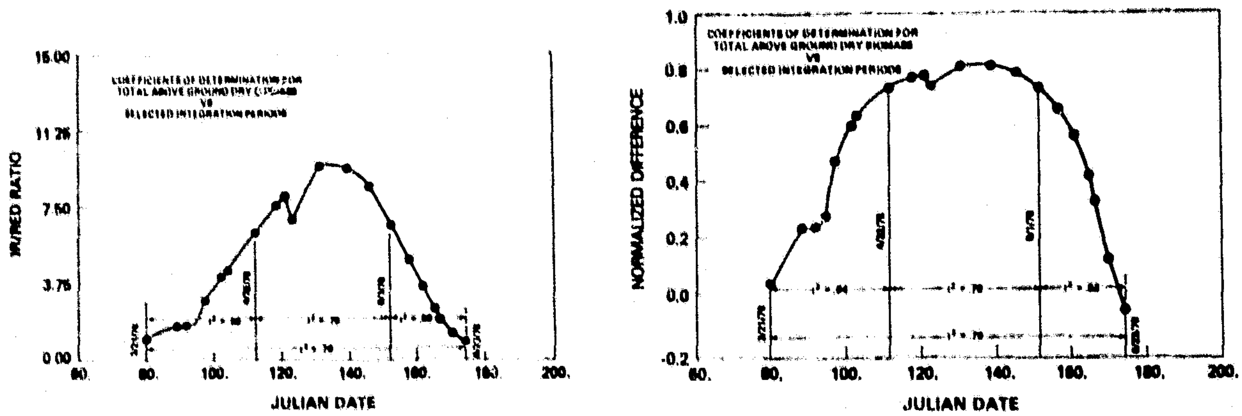

(A) (B)

Figure 5. The (A) IR/red radiance ratio and (B) normalized difference are plotted against Julian date. Coefficients of determination (r^2) were calculated for several time periods by integrating under each curve of the twenty plots and correlating the integrated areas to the total dry matter accumulation. See also fig. 6.

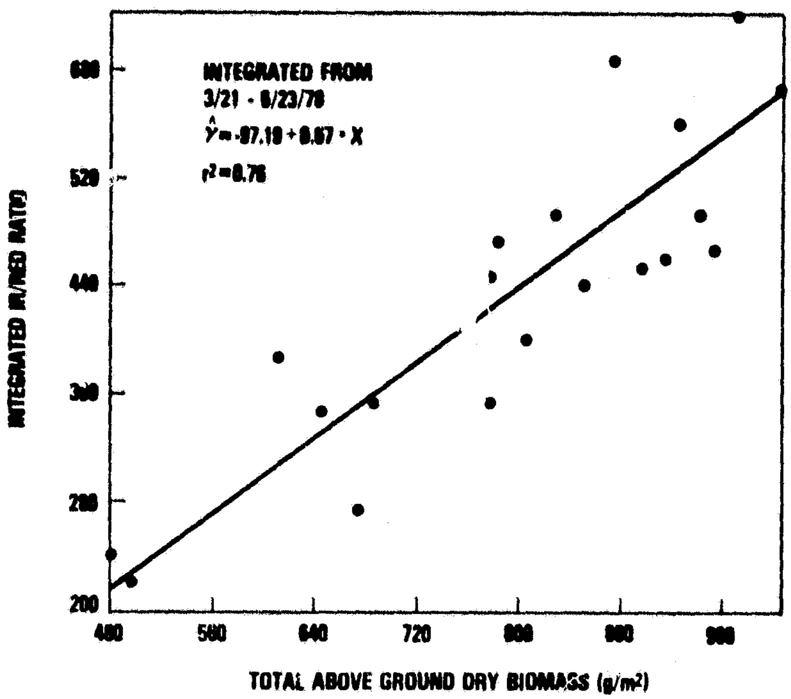

(A)

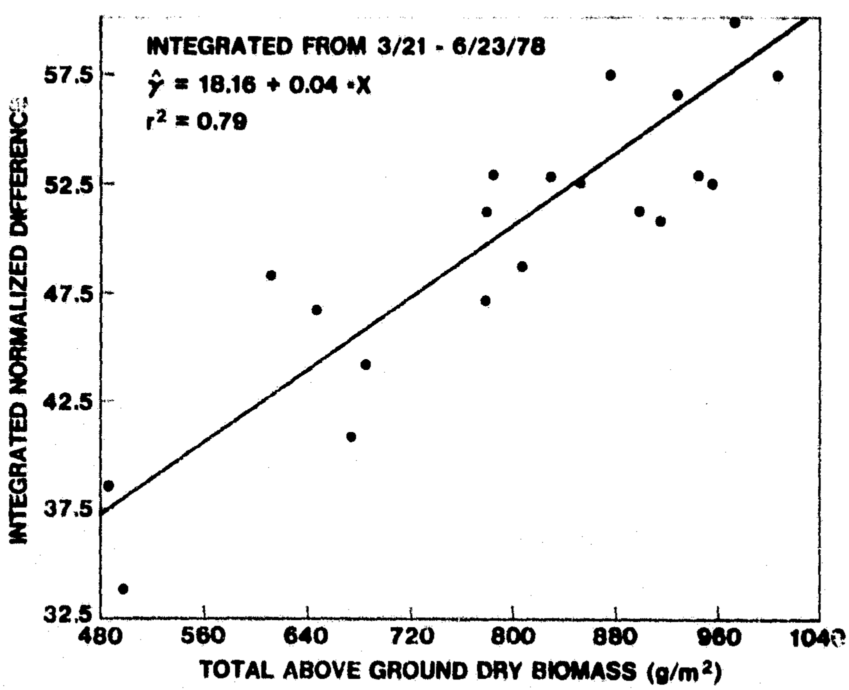

(B)

Figure 6. The integrated (A) IR/red radiance ratio and (B) normalized difference plotted against total above ground dry matter accumulation. The integrated values were formed by computing the area under each curve for the 20 plots sampled, respectively. See also fig. 5.

species in the same stage of growth that are not having water-uptake deficiencies (Coleman, 1975). Considering only the above-ground total accumulation of dry matter thus introduces a slight error. It is likely that more significant correlations would result between the spectral data and total below-ground and above-ground dry matter accumulation. However, determination of below-ground total accumulation of dry matter is extremely tedious, laborious, and time consuming because it includes digging and washing of roots, and such data are not usually available. Thus we confined our study to the above-ground total accumulation of dry matter.

We feel that our results showing clear relationships between spectral values and dry-matter accumulation are sufficiently encouraging to warrant use of a similar technique on other plant communities. We acknowledge that our results were obtained from small experimental plots (2 × 3 m) in single field, and that the data used herein represent a narrow range of total dry-matter accumulation (i.e., in these plots the planting density, soil types, microclimate, etc., were very similar). However, the validity of this method for monitoring dry-matter accumulation and its extension to other herbaceous vegetation can easily be tested with hand-held radiometers in a variety of ecological settings.

LARGE SCALE APPLICATION OF THESE FINDINGS

The research results reported herein were from small experimental plots using ground-collected spectral data. Global or regional assessment of net primary production, however, can only be accomplished with satellite observation systems. Earth resource satellites alone allow for the synoptic, repetitive, and sun-synchronous coverage necessary for large-area assessment of net primary production. We will now discuss the capabilities of existing and proposed satellite systems for assessing net primary production via remotely sensed spectral data.

The basic requirements of any satellite system for achieving the assessment of net primary production involve frequent data collection, suitable red and photographic infrared spectral bands, suitable radiometric resolution, and suitable spatial resolution. Definition of the frequency of data collection is evident from the experimental data presented in this report. An important prerequisite for successful satellite application of this technique is to have frequently collected spectral data (4-10 days). Spectral band selection is rather straightforward and involves the choice of only two bands with maximum background spectra–green vegetation spectral contrasts and simultaneously avoiding or minimizing atmospheric transmission/absorption effects while maintaining a high NE$\Delta\rho$. A band in the red and a band in photographic infrared are suggested after Tucker (1979) as are 256 quantizing levels. Suitable spatial resolution, however, poses a more difficult question.

The spatial resolution requirement(s) depend to a large extent upon the information needs of the user. For regional or large area studies, a larger instantaneous field of view (IFOV) is desirable. It would be impractical, for example, to attempt to use Landsat-MSS data for any large area assessment of net primary productivity. The 80 m IFOV is simply too small and this results in a substantial volume of data to be processed, stored, etc. For a regional inventory, a 200-1000 m IFOV would be desirable. This larger IFOV would result in a dramatic decrease in the amount of data from the area in question and, accordingly, more data could be collected. A small IFOV is not required for our proposed purpose and would actually be a liability.

It is desireable to have the maximum swath width possible without introducing significant atmospheric variability into the spectral data as a result of atmospheric path radiance differences (i.e., nadir vs. extreme side scans). In addition, the total field of view of the satellite sensor system is restricted by plant canopy bidirectional effects. For these reasons, it will be necessary to restrict the half angle field of view of the proposed satellite sensor system to ~10°. For an orbital altitude of ~900km, this results in a maximum swath-width of ~300 km.

UTILITY OF EXISTING AND PROPOSED SATELLITE SYSTEMS

The existing and proposed satellite systems which could be employed for conducting regional large area net primary production studies fall into two main categories. The Landsat MSS, Landsat-D's thematic mapper, and the French (CNES) SPOT satellites all are primarily earth resource satellites and have spatial resolutions less than ~80m (80m, 30m, and 20m, respectively, in the spectral mode).

The other group includes Nimbus-F's coastal zone color scanner (CZCS) and the TIROS-N-NOAA AVHRR instruments with spatial resolutions of 825m and 1100m, respectively. Several pertinent characteristics of each of these satellite systems are listed in Table 5.

Table 5
Satellite System Parameters for Instruments which Could be of Possible Use for Providing Net Primary Production Information

Satellite Systems	Appropriate Spectral Bands (μm)	IFOV (m)	Swath Width (km)	Orbital Alt. (km)	Equatorial Crossing Time (LST) A= Ascending D = Descending
SPOT (CNES)*	0.61-0.69 0.79-0.90	20	117	822	1030-D
TM (Landsat-D)**	0.63-0.69 0.76-0.90	30	180	716	0930-D
MSS	0.6-0.7 0.7-0.8 or 0.8-1.1	80	180	919	0930-D
CZCS (NIMBUS-7)	0.660-0.680 0.700-0.800	825	1566	955	1200-A 2400-D
†$AVHRR_1$***	0.55-0.90 0.725-1.10	1100	horizon to horizon	833	0900-D 1500-A
$AVHRR_2$****	0.55-0.68 0.725-1.10	1100	horizon to horizon	833	0730-D 1500-A

*Scheduled for launch in 1983.
**Scheduled for launch in 1981 or 1982.
***AVHRR on TIROS-N.
****AVHRR on NOAA series; The five channel instruments have a slight change to the red band of 0.58-0.68 μm.
†The 0.55-0.90 μm band on TIROS-N is not applicable for monitoring primary productivity because of its bandwidth.

It is apparent from Table 5 that a satellite system similar to the one we propose does not, nor is currently planned to exist in the immediate future. We propose that a relatively coarse spatial resolution earth observation series of satellites be seriously considered which would have at least a red band and photographic infrared band for the expressed purpose of monitoring terrestrial net primary production. Three of these "primary production satellites" in orbit simultaneously would result in 4-5 day repeat coverage and would provide a necessary and currently missing input into our understanding of the terrestrial phytomass and its relationship to the carbon dioxide question. In addition, primary production data as we propose would have applications for other large-area ecological purposes such as deforrestation, drought analysis, desertification, acid rain, and any other occurrences which adversely affect primary production over large areas. Evaluation of our proposal could be undertaken using $AVHRR_2$ data from NOAA-B which is scheduled for launch in May, 1980.

CONCLUSIONS

1. Red and photographic infrared spectral data were found to be highly related to canopy vigor of winter wheat and its response to rainfall after mild drought.
2. The IR/red radiance ratio and the normalized difference integrated over spectral sampling dates were found to be strongly related to above-ground total accumulation of dry matter in winter wheat.
3. A satellite system is proposed to allow large-area assessment of net primary production or total dry matter accumulation. This information would have immediate use in addressing some of the questions associated with the role of the terrestrial phytomass in the carbon dioxide cycle. In addition, this information would provide large-area primary production data for monitoring desertification, drought, deforestation, acid rain, and many other occurrences which adversely affect plant growth and development.

ACKNOWLEDGMENTS

We thank the following people for help in the collection of data in the field: Chris Justice, Dan Kimes, Donna Strahan, Diana Crowley, Maryann Karinch, Charley Walthall, Josette Pastor, Jelle Hielkema, Steve Bogash, Don Friedman, Bill Jones, and Bill Wigton. We thank Freeman Smith for the loan of the instrument.

REFERENCES

Aase, J. K. and F. H. Siddoway. 1980. Spring wheat yield estimates from spectral reflectance measurements. Environmental Management (under consideration).

Anderson, N. R. and A. Malahoff (eds.). 1977. The Fate of Fossil Fuel CO_2 in the Oceans. Plenum Press, New York.

Anuta, P. E. and R. B. MacDonald. 1971. Crop Surveys from multiband satellite photography. Remote Sensing Environ. 2:53-67.

Ashley, M. D. and J. Rea. 1975. Seasonal vegetation differences from ERTS imagery. Photogramm. Engr. and Remote Sensing 41(6):713-719.

Atjay, G. L., P. Detner, and P. Duvigneaud. 1979. Terrestrial primary production and photomass. In: The Global Carbon Cycle, B. Bolin, E. T. Degens, S. Kempe, and P. Detner (eds.), Chapter 5, SCOPE Report No. 13, John Wiley and Sons, New York.

Baes, D. F., H. E. Goeller, J. S. Olson, and R. M. Rotty. 1976. The Global Carbon Dioxide Problem. Oak Ridge National Laboratory ORNL 5191, 78 pp.

Bauer, M. E. 1975. The role of remote sensing in determining the distribution and yield of crops. In: Advances in Agronomy (N. C. Brady, Ed.), Academic Press, New York, 2:271-304.

Bauer, M. E., J. E. Cipra, P. E. Anuta, and J. E. Etheridge. 1979. Identification and area estimates of agricultural crops by computer classification of Landsat multispectral scanner data. Remote Sensing Environ. 8(1):77-92.

Bizzell, R., F. Hall, A. Feiveson, M. Bauer, M. Davis, W. Malila, and D. Rice. 1975. Results from the crop identification technology assessment for remote sensing (CITARS) project. Proc. Tenth Int. Symp. Remote Sens. Envir., Ann Arbor, MI, October 6-10 pp. 1189-1198.

Blair, B. O. and M. F. Baumgardner. 1977. Detection of the green and brown wave in hardwood canopy covers using multidate multispectral data from Landsat-1. Agron. J. 69; 808-811.

Bohn, J. L. 1976. Estimate of organic carbon in world soils. Soil Sci. Soc. Amer. J., 40:468-470.

Bolin, B. 1970. The carbon cycle. Scientific American 223:125-132.

Bolin, B. 1977. Changes of land biota and their importance for the carbon cycle. Science, 196:613-615.

Bolin, B., E. T. Degens, S. Kempe, and P. Ketner. 1979. The Global Carbon Cycle, SCOPE Report No. 13, John Wiley and Sons, New York.

Carneggie, D. M., S. D. deGloria, and R. N. Colwell. 1974. Usefulness of ERTS-1 and supporting aircraft data for monitoring plant development and range conditions in California's annual grassland. BLM Final Report 53500-CT3-266(N).

Coleman, D. C. 1975. A review of root production processes and their influence on soil biota in terrestrial ecosystems. In: The Role of Terrestrial and Aquatic Organisms in Decomposition Processes. Blackwell Sci. Pub., London.

Colwell, J. E 1974. Vegetation canopy reflectance. Remote Sensing Environ. 3:175-183.

Colwell, J. E., D. P. Rice, and R. F. Nalepka. 1977. Wheat yield forecasts using Landsat data. In: Proc. of the 11th Int. Symp. on Remote Sensing Environ., University of Michigan, Ann Arbor, p. 1245-1254.

Deering, D. W., J. W. Rouse, R. H. Haas, and J. A. Schell. 1975. Measuring forage production of grazing units from Landsat MSS data. Proc. 10th Int. Symp. on Remote Sensing Environ. pp. 1169-1178.

Frasier, R. S. 1975. In: Manual of Remote Sensing. American Soc. of Photogram., Falls Church, Va., pp. 181-234.

Gates, D. M., H. J. Keegan, J. C. Schleter, and V. P. Weidner. 1965. Spectral properties of plants. Appl. Optics 4:11-20.

Hay, C. M. 1974. Agricultural inventory techniques with orbital and high-altitude imagery. Photogramm. Eng. 40:1283-1293.

Holben, B. N., C. J. Tucker, and C. J. Fan. 1980. Assessing leaf area and leaf biomass with spectral data. Photogram. Engr. and Remote Sensing (in press).

Jordan, C. F. 1969. Derivation of leaf area index from quality of light on the forest floor. Ecology 50(4):663-666.

Keeling, C. D. 1973. Industrial production of carbon dioxide from fossil fuels and limestone. Tellus 25:174-198.

Keeling, C. D., J. A. Adams, C. A. Ekdahl, and P. R. Guenther. 1976a. Atmospheric carbon dioxide variations at the South Pole. Tellus 28:552-564.

Keeling, C. D., R. B. Bacastow, A. E. Bainbridge, C. A. Ekdahl, P. R. Guenther, L. S. Waterman, and J. F. S. Chin. 1976b. Atmospheric carbon dioxide variations at Mauna Loa Observatory, Hawaii. Tessus, 28:538-551.

Kettig, R. L. and D. A. Landgrebe. 1976. Classification of multispectral image data by extraction and classification of homogeneous objects IEEE Trans. Geos. Elect. 14:19-25.

Kumar, R. and L. F. Silva. 1977. Separability of agricultural cover types by remote sensing in the visible and infrared wavelength regions. IEEE Trans. Geos. Elect. 15:42-49.

Lemon, E. 1977. The land's response to more carbon dioxide. In: The Fate of Fossil Fuel CO_2 in the Oceans, N. R. Andersen and A. Malahoff (eds.), pp. 97-130, Plenum Press, New York.

Kimes, D. S., B. L. Markham, C. J. Tucker, and J. E. McMurtrey. 1980. Temporal relationships between spectral response and agronomic values of a corn canopy. NASA/GSFC Tech. Memo (in prep.).

Knipling, E. B. 1970. Physical and physiological basis for the reflectance of visible and near infrared radiation from vegetation. Remote Sensing of Environ. 1(3):115-119.

MacDonald, R. B., M. E. Bauer, R. D. Allen, J. W. Clifton, J. D. Erickson, and D. A. Landgrebe, 1972, Results of 1971 Corn Blight Experiment. Proc. Eighth Int. Symp. Remote Sens. Environ., Ann Arbor, MI, October 2-6, pp. 157-190.

MacDonald, R. B. and F. G. Hall. 1977. LACIE: A look to the future. In: Proc. of the Eleventh Int. Symp. Remote Sens. Envir., Ann Arbor, Mich., April 25–29, pp. 429-465.

Maxwell, E. L. 1976. Multivariate system analysis of multispectral imagery. Photogram. Engr. and Remote Sensing 42(9):1173-1186.

Miller, L. D. and D. L. Williams, 1978. Monitoring forest canopy alteration around the world with digital analysis of Landsat imagery. NASA/GSFC Tech. Memo. 80340.

Morian, S. A. and D. L. Williams. 1975. Wheat production estimates using satellite images. Agron. J. 67:361-364.

Pearson, R. L. and L. D. Miller. 1972. Remote mapping of standing crop biomass for estimation of the productivity of the shortgrass prairie. In: Proc. 8th International Symposium on Remote Sensing of Environment, Univ. of Michigan, Ann Arbor, pp. 1357-1381.

Pearson, R. L., L. D. Miller, and C. J. Tucker, 1976a. Hand-held spectral radiometer to estimate gramineas biomass. Appl. Optics 15(2):416-418.

Pearson, R. L., C. J. Tucker, and L. D. Miller. 1976b. Spectral mapping of shortgrass prairie biomass. Photogram. Engr. and Remote Sensing 42(3):317-323.

Pinter, P. J., Jr., R. D. Jackson, S. B. Idso, and R.J. Reginato. 1979. Multidate spectral reflectances as predictors of yield in water stressed small grains. Submitted to Nature.

Richardson, A. J. and C. L. Wiegand. 1977. Distinguishing vegetation from soil background information. Photogram. Engr. and Remote Sensing 43(12):1541-1552.

Rodin, L. E., N. I. Bazilevich, and N. N. Rozow. 1975. Productivity of the world's main ecosystems. In: Productivity of World Ecosystems, National Academy of Sciences, Washington, D. C. pp. 13-26.

Rotty, R. M. 1977. Global carbon dioxide production from fossil fuels and cement: A. D. 1950-A. D. 2000. In: N. R. Andersen and A. Malahoff, Eds. The Fate of Fossil Fuel CO_2 in the Oceans. Plenum Press, N. Y.

Rotty, R. 1978. The atmospheric CO_2 consequences of heavy dependence on coal. In: Carbon Dioxide, Climate and Society. Pergamon Press, N. Y. 332 pp.

Rouse, J. W., R. H. Haas, J. A. Schell, and D. W. Deering. 1973. Monitoring vegetation systems in the great plains with ERTS. Third NASA ERTS Symposium, NASA SP-351 I:309-317.

SCEP 1979. Man's impact on the global environment: Assessment and recommendations for action. In: Study of Critical Environmental Problems, Cambridge: MIT Press.

Schlesinger, W. H. 1979. The world carbon pool in soil organic matter. A source of atmospheric CO_2? Scope CO_2 Conf., Woods Hole, Mass. May 5-12, 1979.

Steiner, D. 1970. Time dimension for crop surveys from space. Photogram. Eng. 36:187-194.

Stuiver, M. 1978. Atmospheric CO_2 increase related to carbon reservoir changes. Science 199: 253-260.

Swain, P. H. 1972. Pattern Recognition: A basis for remote sensing data analysis. Information Note 111572, Laboratory for Applications of Remote Sensing, Purdue University, West Lafayette, IN.

Thompson, D. R. and O. A. Wehmanen. 1979. Using Landsat digital data to detect moisture stress. Photogram. Engr. and Remote 45(2):201-207.

Tucker, C. J. 1977. Spectral estimation of grass canopy variables. Remote Sensing Environ. 6(1):11-26.

Tucker, C. J. 1979. Red and photographic infrared linear combinations for monitoring vegetation. Remote Sensing Environ. 8(2):127-150.

Tucker, C. J. and E. C. Maxwell. 1976. Sensor design for monitoring vegetation canopies. Photogram. Engr. and Remote Sensing. 42(11):1399-1410.

Tucker, C. J., L. D. Miller, and R. L. Pearson. 1975. Shortgrass prairie spectral measurements, Photogram. Engr. and Remote Sensing. 41(9):1157-1162.

Tucker, C. J., J. H. Elgin, and J. E. McMurtrey. 1980a. Relationship of crop radiance to alfalfa agronomic values. Int. J. Remote Sensing 1(1):(in press).

Tucker, C. J., B. N. Holben, J. H. Elgin, and J. E. McMurtrey, 1980b. Relationship of spectral data to grain yield variation. Photogram. Engr. and Remote Sensing. 46(in press).

Tucker, C. J., J. H. Elgin, and J. E. McMurtrey. 1979a. Temporal spectral measurements of corn and soybean crops. Photogram. Engr. and Remote Sensing 45(5):600-608.

Tucker, C. J., J. H. Elgin, J. E. McMurtrey, and C. J. Fan. 1979b. Monitoring corn and soybean crop development with hand-held radiometer spectral data. Remote Sensing Environ. 8(2):237-248.

Whittaker, R. H. and G. E. Likens. 1975. The biosphere and man. In: Primary Productivity of the Biosphere, H. Lieth and R. H. Whittaker (eds.), Ecological studies, 14, Springer-Verlag, New York.

Wiegand, C. L., A. J. Richardson, and E. T. Kanemasu. 1979. Leaf area index estimates for wheat from Landsat and their implications for evapotranspiration and crop modeling. Agron. J. 71: 336-342.

Williams, J. 1978. Carbon Dioxide, Climate, and Society. Pergamon Press, New York, 332 pp.

Woodwell, G. M. and R. A. Houghton, 1977. Biotic influences on the world carbon budget. In: Global Chemical Cycles and their Alterations by Man, W. Stumm (ed.) Dahlem Konferenzen, Berlin pp. 61-72.

Woodwell, G. M. and E. V. Pecan (eds.). 1973. Carbon and the Biosphere, USAEC, Technical Information Center, Springfield, VA. 392 pp.

Woodwell, G. M., R. H. Whittaker, W. A. Reiners, G. E. Likens, C. C. Delwiche, and D. B. Botkin. 1978. The biota and the world carbon budget. Science, 199:141-146.

Woodwell, G. M. 1978. The carbon dioxide question. Sci. Am. 138(1):34-43.

Woolley, J. T. 1971. Reflectance and transmittance of light by leaves. Plant Physiol. 47:656-662.